Taylor & Francis
Taylor & Francis Group

REPORT

Novel multispecific heterodimeric antibody format allowing modular assembly of variable domain fragments

Timothy J. Egan[a,b], Dania Diem[a], Richard Weldon[a], Tessa Neumann[a], Sebastian Meyer[a], and David M. Urech[a]

[a]Numab AG, Wadenswil, Switzerland; [b]Cartilage Engineering & Regeneration Lab, Department of Health, Science & Technology, The Swiss Federal Institute of Technology (ETH), Zurich, Switzerland

ABSTRACT

Multispecific antibody formats provide a promising platform for the development of novel therapeutic concepts that could facilitate the generation of safer, more effective pharmaceuticals. However, the production and use of such antibody-based multispecifics is often made complicated by: 1) the instability of the antibody fragments of which they consist, 2) undesired inter-subunit associations, and 3) the need to include recombinant heterodimerization domains that confer distribution-impairing bulk or enhance immunogenicity. In this paper, we describe a broadly-applicable method for the stabilization of human or humanized antibody Fv fragments that entails replacing framework region IV of a $V_\kappa 1/V_H 3$-consensus Fv framework with the corresponding germ-line sequence of a λ-type V_L chain. We then used this stable Fv framework to generate a novel heterodimeric multispecific antibody format that assembles by cognate V_L/V_H associations between 2 split variable domains in the core of the complex. This format, termed multispecific antibody-based therapeutics by cognate heterodimerization (MATCH), can be applied to produce homogeneous and highly stable antibody-derived molecules that simultaneously bind 4 distinct antigens. The heterodimeric design of the MATCH format allows efficient in-format screening of binding domain combinations that result in maximal cooperative activity.

Introduction

Recombinant antibody-based molecules that specifically recognize multiple, distinct targets (e.g., multispecific antibodies) have enabled the realization of novel mechanisms of action that aim to improve therapeutic efficacy and safety.[1-6] For instance, monotherapies that concomitantly engage multiple targets have been shown to synergistically interfere with signaling pathways in a manner superior to even combination therapies consisting of monospecific antibodies targeting the same collection of antigens.[7-9] In addition, multispecific antibody therapeutics can be endowed with paratopes that promote enhanced molecular pharmacokinetic properties such as prolonged serum half-life,[10] improved tissue distribution[11-13] and local enrichment.[14]

The marketing approvals of bispecific antibody drugs such as blinatumomab (BLINCYTO®)[15] and catumaxomab (Removab)[16] have validated the therapeutic value of this class of biologics. In addition, more than 30 bispecific antibodies – employing various molecular designs – are currently undergoing clinical development.[17] The next frontier of antibody-based therapeutics appears to be the production and application of higher-order multispecifics (i.e., molecules exhibiting >2 specificities). Indeed, researchers have already described the successful production of trispecific antibodies in TriMAb,[18] triplebody,[19,20] and tribody[21] formats. Additional specificities could, for example, enable higher-avidity binding to target cell populations by promoting the simultaneous

engagement of multiple cell-type-associated antigens.[4] This would theoretically minimize off-target drug interactions, while additional specificities could be added to site-specifically recruit effector cells or enhance drug pharmacokinetics.

Conventional higher-order multispecific antibodies often require inclusion of multimerization domains that result in relatively large protein assemblies.[18,21] This has the drawback of reducing potential drug distribution and tissue penetration,[22] and may lead to unwanted off-target activity.[23] An alternative to such designs would be to simply drive the assembly of multispecifics exclusively through interactions between complementary antibody variable domains, such as in the triplebody format.[19,20] However, the dependable production of such multispecifics relies heavily on the stability of the variable domain pairs, which is typically compromised in the absence of antigen-binding fragment (Fab) constant domains.[24] Such compromised stability could result in local unfolding and the solvent-exposure of aggregation "hot spots," which would then mediate the aggregation of the composite molecule.[25]

Additionally, higher-order multispecific antibodies that are formed by the assembly of 2 non-identical subunits (heterodimeric multispecifics) enable the rapid production and testing of different binding domain combinations by simple permutation of plasmids expressing single subunits, thereby enhancing the efficiency of drug screening. Comparable screening efforts

applied to single-chain or homomultimeric multispecific formats with the same protein-targeting profile would require considerably more cloning steps and consequently increase the time and effort needed to generate them. Improved multispecific antibody screening efficiency would facilitate the identification of cooperative binding-domain specificities and affinities, and such binding-profile optimization in the final format could be critical to eliciting the molecule's intended effects *in vivo*.[26,27]

Currently, the only heterodimeric antibody-based molecules consisting exclusively of variable domains that have been described in the literature are bispecific, such as the diabody[28] format. Two critical factors appear to be complicating the efficient production of variable-domain-only, higher-order heterodimeric multispecifics. These include: 1) impurities in production samples arising from the incorrect assembly of subunits;[29] and 2) protein aggregation resulting from the aggregation propensity of the constituent variable domains. Solutions to these issues appear to necessitate not only a re-design of subunit orientation and subunit association strategies, but also improvements to the stability of variable domain frameworks and the integrity of the variable domain interface.

Here, we first present the development of a novel, broadly-applicable human variable fragment (Fv) framework for the stabilization of antibody variable domains. Based on our interpretation of the literature,[30,31] as well as analysis of crystal structures of different fragment variants originating from the same antibody, we hypothesized that replacement of a κ-derived Fv V_L framework region IV (V_L FW IV) with a germ-line sequence from the corresponding position of a human V_λ domain (known here onward as the "λcap") would improve Fv stability. Our results confirm that the λcap enhances stability of humanized single-chain Fvs (scFvs) displaying both murine and rabbit complementarity-determining region (CDR) sets.

We were then able to incorporate our stable Fv framework into novel heterodimeric multispecific formats whose assembly is driven exclusively by variable domain associations. We termed these the multispecific antibody-based therapeutics by cognate heterodimerization (MATCH) formats. In addition to the limited aggregation propensity of the proof-of-concept MATCH proteins we produced in this study, the structure of the 2 MATCH chains prevents homodimer formation in production samples and limits the potential for non-cognate intra-chain V_L/V_H associations, thus allowing greater flexibility in protein design.

Results

Full framework region IV substitution reduces aggregation propensity and improves thermal stability of a hu4D5–8 (trastuzumab) scFv variant

In order to evaluate the plausibility of V_L FW IV-mediated Fv instability, we overlaid crystal structures, retrieved from the RCSB Protein Data Bank (PDB), of Fab (PDB ID: 1FVD) and Fv (PDB ID: 1FVC) variants of hu4D5–8[32] to determine whether this region might assume an unnatural conformation in the absence of Fab constant domains. Indeed, we observed a considerable structural difference in V_L FW IV between the Fab and the Fv variants (Fig. 1C). Specifically, the absence of Fab constant domains appears to result in the solvent-exposure of a hydrophobic Ile residue at position 147 in V_L FW IV, as well as a skewing of the downstream hydrophilic residues (for the AHo antibody sequence numbering scheme used in this paper, please refer to the work by Honegger et al.[33]). In light of these observations, we produced and compared 2 hu4D5–8 scFv variants, one with the original variable domain sequence (Tras-scFv) and one with a λcap (Tras-scFv-λcap) consisting of
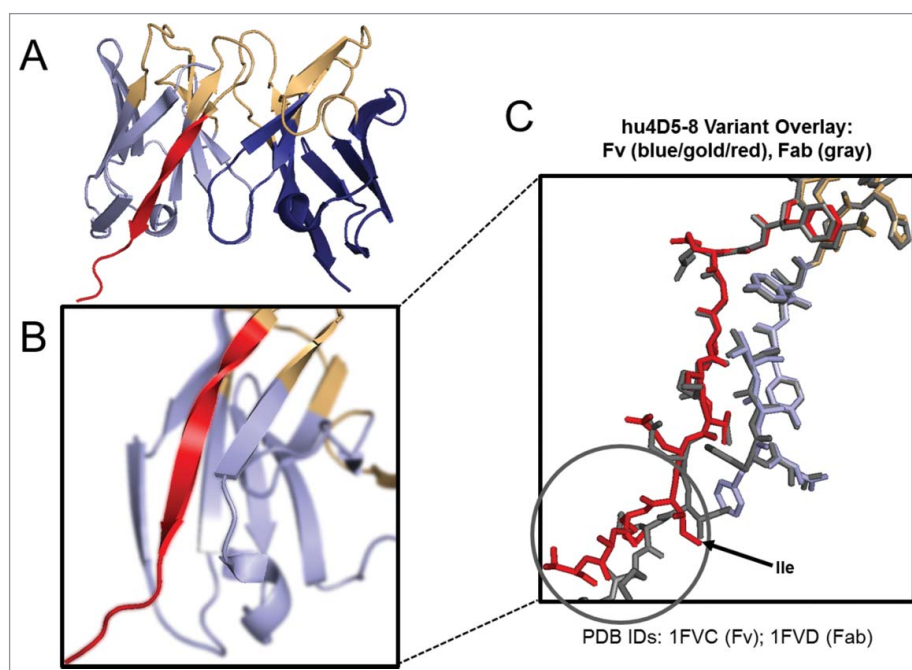
Figure 1. Putative structural change of V_L FW IV in the hu4D5–8 Fv variant. (A) Cartoon visualization of the crystal structure of a hu4D5–8 Fv variant (PDB ID: lFVC) assembled by heterodimerization of the V_L (left half) and V_H (right half) domains. The murine CDR sets are shown in gold, the human Fv acceptor framework is shown in light blue (V_L) and dark blue (V_H) and the location of V_L FW IV is shown in red. (B) View of the hu4D5–8 V_L domain showing the position of the region (vivid) depicted in the overlay in (C) relative to the rest of the V_L domain (blurred). (C) Overlay of the crystal structures of the Fab and Fv variants of hu4D5–8, revealing an apparently unnatural solvent exposure of I147 and skewing of the C-terminal residues in the Fv variant relative to the constant domain-bearing Fab structure.

a λ germ-line sequence (FGGGTKLTVLG) replacing the entire V_κ FW IV. Each scFv was designed with a N-term–V_L–peptide linker–V_H–C-term orientation (peptide linker: $(G_4S)_4$).

We successfully produced both scFvs by refolding from inclusion bodies (Fig. 2A-B). However, after applying affinity capture and size exclusion chromatography (SEC) polishing to both proteins, disparate levels of scFv-monomer content (% of total protein content) were obtained – 97.4% and 73.3% for Tras-scFv-λcap monomer (0.648 mg/mL) and Tras-scFv monomer (0.780 mg/mL), respectively. This provided an early indication that the λcap renders the scFv less prone to aggregation (Fig. 2B). Meanwhile, both antibodies exhibited comparable affinities for recombinant human HER2 (Table 1), suggesting that the λcapped framework can be applied to stabilize a CDR set derived from a V_κ-bearing IgG. Additionally, differential scanning fluorimetry (DSF) revealed a higher melting temperature ($n = 2$, unpaired Student's t test: $p < 0.05$) of Tras-scFv-λcap (mean Tm°C ± SD: 71.2 ± 0.1) relative to Tras-scFv (69.9 ± 0.1), indicating a modest increase in thermal stability of λcapped protein (Fig. 2C).

Finally, because oligomerization of scFvs is largely concentration-dependent, we generated scFv aliquots at escalating protein concentrations by centrifuging the protein samples through filters with a 5 kDa molecular weight cut-off (MWCO). We then analyzed the samples to determine whether the scFvs exhibited a disparate propensity toward concentration-induced aggregation. The oligomer content in Tras-scFv samples was considerably higher than that of Tras-scFv-λcap at all concentrations (Fig. 2D), plateauing at ~10 mg/mL with an oligomer content of ~55–60%. The oligomer content of Tras-scFv-λcap, meanwhile, appears to be <25% at ~10 mg/mL, and the percentage of oligomer in samples did not exceed ~46% up to a concentration of ~30 mg/mL.

λcap substitution enhances the stability of a human $V_\kappa 1/V_H 3$ consensus scFv acceptor framework used to humanize an anti-tumor necrosis factorα rabbit CDR set

While our initial data supported a considerable stabilizing effect of the λcap in the context of hu4D5–8 scFv variant, it is important to consider that while the framework in the hu4D5–8 Fv variant is highly homologous to the $V_\kappa 1/V_H 3$ consensus,[31] it differs from a full human consensus by 6
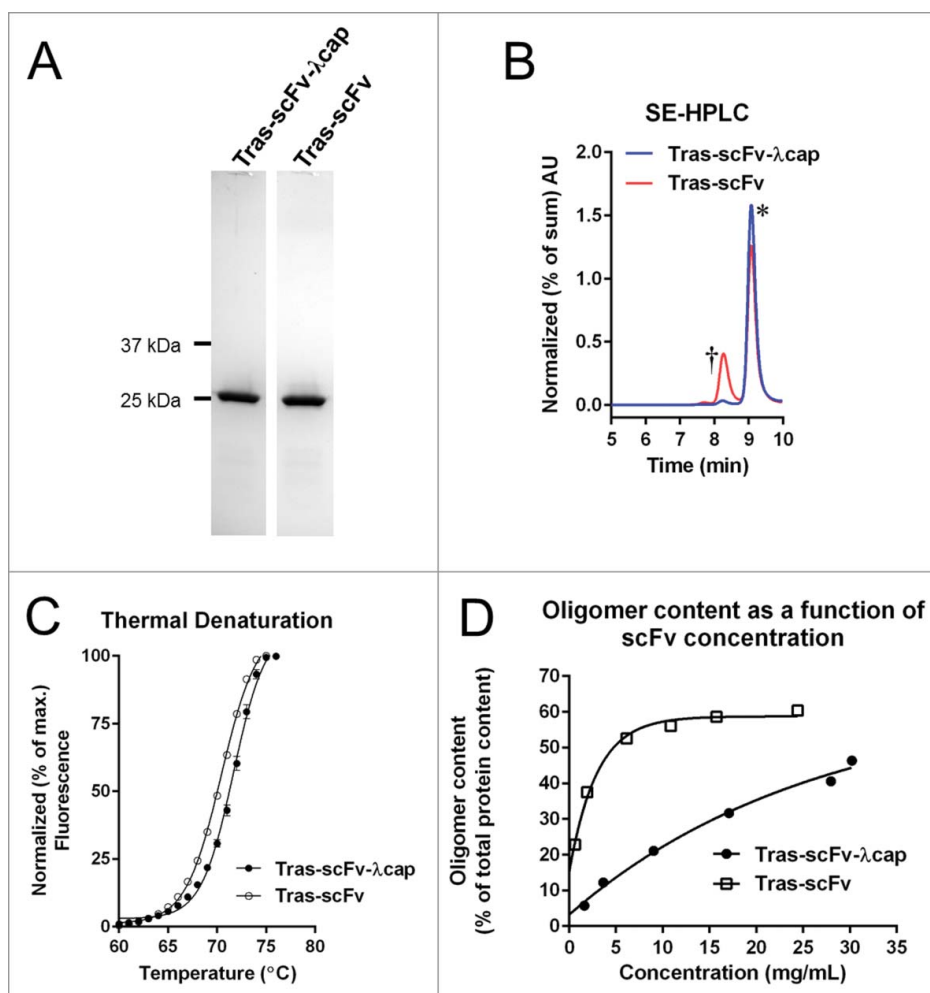
Figure 2. Improved stability and monomer content of λcapped hu4D5–8 scFv variant. (A) Coomassie-stained SDS-PAGE gel reveals that purified samples of both scFv variants travel as discrete bands with anticipated electrophoretic mobility and without any detectible impurities. (B) SE-HPLC chromatograms of purified protein samples with the lowest multimer content for each respective scFv variant; scFv monomer (*) and scFv dimer (†) peaks are indicated. (C) Thermal unfolding curves of each scFv variant fitted with the Boltzmann equation to data points (n=2 ; mean ± SD) generated in a DSF assay. (D) Graph depicting concentration-induced aggregation of the respective scFv variants.

Table 1. Antigen-binding kinetics of anti-HER2 scFv variants as determined by SPR analysis.

	k_{on} (1/M·s)	k_{off}	K_D (M)
Tras-scFv	3.81×10^5	5.30×10^{-5}	1.39×10^{-10}
Tras-scFv-λcap	2.70×10^5	5.75×10^{-5}	2.14×10^{-10}

residues (V_L: G84R; V_H: S55A, R81A, N83T, L88A, A106S). Also, while murine CDR sets (such as those displayed by hu4D5–8) are more commonly observed in therapeutic and clinical applications at present, rabbit CDR sets are increasingly considered more desirable[34] as they exhibit greater sequence diversity,[35] facilitating the selection of high-affinity antibodies. With this in mind, we sought to evaluate the use of the λcap in a full V_κ1-V_H3 consensus framework in combination with previously described rabbit anti-tumor necrosis factor (TNF)α CDR sets[36] introduced by CDR grafting using the definitions employed by Borras.[37] To that end, we again designed 2 scFvs with (aTNFα-scFv-λcap) and without (aTNFα-scFv) the λcap (Fig. 3).

As confirmed by SDS-PAGE and SE-HPLC, we successfully purified both scFvs (Fig. 4A-B) to comparable quality, and surface plasmon resonance (SPR) analysis (Fig. 4C) confirmed the immune-reactivity of the CDR, with each molecule exhibiting comparable affinities for human TNFα (Table 2). We again observed a consistent improvement in the melting temperature ($n = 3$, unpaired Student's t test: p < 0.01) of the λcapped scFv relative to its full-consensus counterpart (mean Tm°C ± SD: aTNFα-scFv-λcap = 63.5 ± 0.1; aTNFα-scFv = 62.5 ± 0.2) in DSF assays (Fig. 5A).

Moreover, aggregation propensity was substantially reduced by the λcap substitution, as evidenced by the considerable differences in the monomer content of protein samples we observed after concentration and during storage (Fig. 5B-C). Two-week storage at 37°C resulted in monomer losses of 0.03% ± 0.05% and 16.7% ± 0.1% in 1 mg/mL samples ($n = 3$) of aTNFα-scFv-λcap and aTNFα-scFv, starting from monomer contents (at day 0) of 98.0% and 93.5%, respectively. After 2-week storage, 10 mg/mL samples of aTNFα-scFv-λcap were composed of 83.7% ± 0.1% (37°C; $n = 3$) or 93.2% (4°C;

$n = 1$) monomeric protein, whereas comparator aTNFα-scFv samples consisted of 35.8% ± 0.3% (37°C; $n = 3$) or 35.7% ± 0.1% (4°C; $n = 3$) scFv-monomer. These results illustrate the substantial production advantages conferred by this fully human substitution of V_L FW IV. Additionally, this enhanced protein stability should translate into a reduced risk of immunogenicity and more dependable reactivity *in vivo*, pointing to considerable therapeutic advantages.[38-40]

Stability-enhanced Fv frameworks used for the construction of functional MATCH formats

We were able to consistently apply λcap technology to V_κ1/V_H3-consensus-derived frameworks to produce functional and stable, humanized Fv modules derived from a discovery platform for rabbit monoclonal antibodies by simple CDR engraftment.[37,41,42] This technology was incorporated in a variety of antibody-based designs, such as scFv,[43] single-chain diabody (scDb)[44] and Fab-scFv[21] formats, with every molecule showing limited aggregation propensity (data not shown). The finding that λcapping V_κ1-V_H3 scFvs attenuates protein aggregation during sample storage suggested to us that this novel, chimeric framework strengthens the V_L/V_H domain interface, while the preservation of antigen-affinities after humanization of V_κ-bearing IgGs confirms the compatibility of this λ-derived substitution with κ-like CDR sets.

Since it is well described that biophysical properties of variable domains can be transferred between different antibody formats,[45] we were motivated to combine these highly stable functional Fv modules in a single molecule to produce a novel class of heterodimeric, tetraspecific antibody derivatives whose assembly is exclusively driven by interactions between cognate variable domains on each protein subunit. Such a design would obviate the need for functionally irrelevant[2] or undesirable dimerization domains, which would normally confer distribution-impairing bulk, the potential for off-target activity, and, possibly, immunogenicity.

Our MATCH concept, as depicted in Fig. 6A-B, requires that the dimer subunits consist of a core of 2 split variable domain pairs,
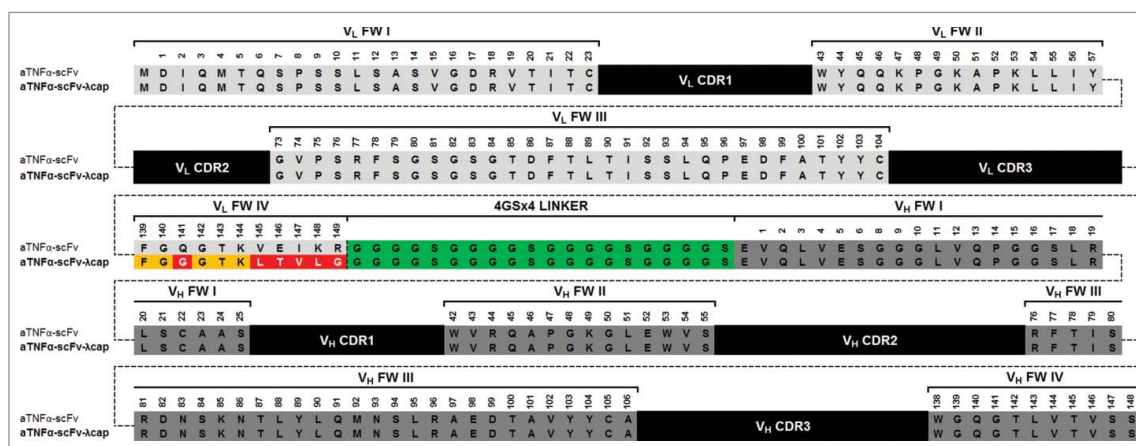
Figure 3. Amino-acid sequence of the V_κ1-V_H3-consensus frameworks with and without the λcap, which were used to humanize the rabbit antibodies, aTNFα-scFv and aTNFα-scFv-λcap, respectively. Differences in the V_L FW IV positions are colored in red. The amino acids are numbered according to the AHo numbering scheme introduced by Honegger & Plückthun.[64]
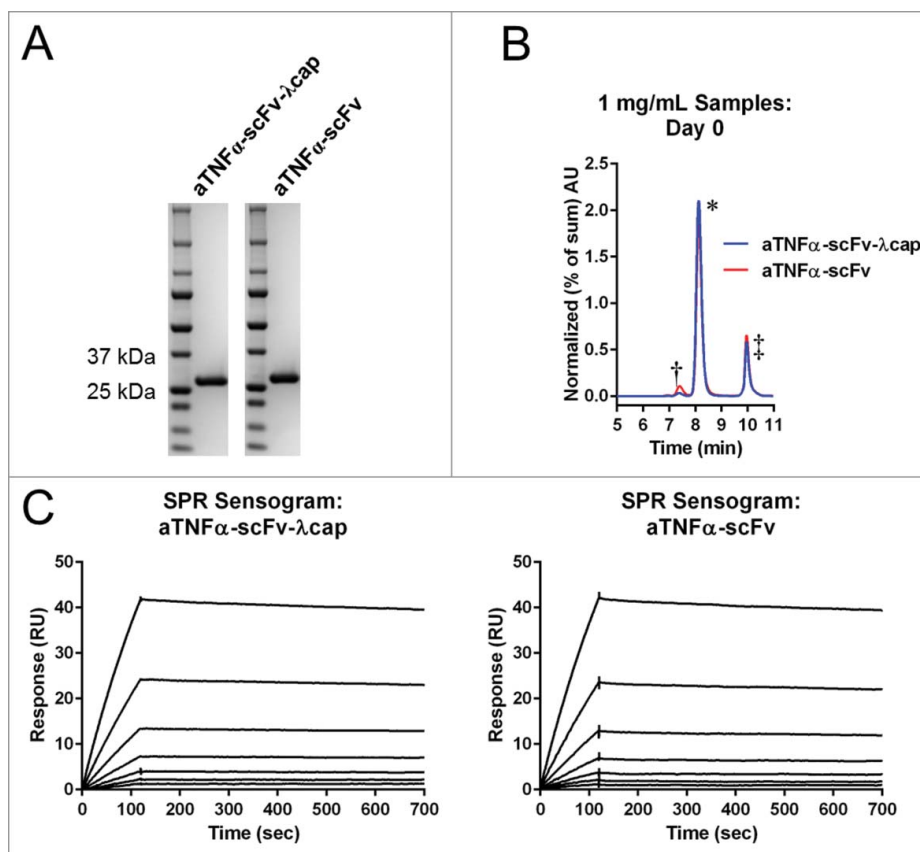
Figure 4. Successful production of pure, immune-reactive, monomeric aTNFα-scFv-λcap and aTNFα-scFv. (A) Coomassie-stained SDS-PAGE gel reveals successful purification of both scFvs. (B) SE-HPLC chromatograms of 1 mg/mL samples of each scFv, revealing comparable sample-quality at day 0 of storage-stability studies; scFv monomer (*), scFv dimer (†) and buffer matrix (‡) peaks are indicated. (C) Sensorgrams generated by SPR analysis by injecting 0.70 – 90 nM of each respective scFv over channels on a sensor chip displaying immobilized, recombinant human TNFα.

each respective subunit possessing either 2 V_L domains or 2 V_H domains positioned in tandem, thereby driving heterodimerization of the 2 protein chains. The dimer-forming tandem variable domains on the respective MATCH chains can be organized in either the same (parallel, Fig. 6A) or reverse (antiparallel, Fig. 6B) N-term–C-term orientation as their counterpart chain, with traditional co-expression in mammalian cells providing adequate conditions for self-assembly (see Supplementary Data, Table 1, for more details). To some extent, this arrangement of the dimer-forming split variable domains in the MATCH subunits resembles the orientation of the dual-variable-domains contained in the constant-domain-bearing DVD-Ig[46] (parallel MATCH) and CODV-Ig[47] (antiparallel MATCH) formats.

Combining a selection of 4 rabbit antibodies humanized with a λcapped $V_\kappa 1/V_H 3$ Fv scaffold, we applied our MATCH concept to generate both parallel (pMATCH) and antiparallel (apMATCH) tetraspecific heterodimers in a proof-of-concept study with therapeutically-nonsensical specificities for human TNFα, CD3ε, IL-5R, and IL-23R (Fig. 6C). In pMATCH, we included a lengthier, 15 amino-acid linker (compared to 6–8 amino acids in other MATCH

proteins) between the heterodimer-forming, split variable domains on each MATCH chain in order to assess the design flexibility these formats can accommodate. Additionally, we surmised that the antiparallel MATCH formats would be amenable to the introduction of a disulfide bridge by addition of a Gly-Ser-Cys sequence at the C-terminal end of each MATCH chain. This was based on our evaluation of juxtaposed scFv models that suggested the close approximation of the MATCH subunits' C-termini in the heterodimer in our antiparallel (but not parallel) formats. This additionally provided us with a convenient means to visualize and confirm dimerization, simply by staining SDS-PAGE gels displaying MATCH proteins that were denatured under non-reducing conditions. Specifically for this purpose, we generated apMATCH-diS (Fig. 6C), whose MATCH chains are identical to those of apMATCH but with the added disulfide bridge-forming feature.

The successful expression of pMATCH, apMATCH and apMATCH-diS protein chains was confirmed by SDS-PAGE and SE-HPLC analysis (Fig. 7A & D). Using supernatants from transiently-transfected mammalian cells, we were able to produce between 3.4 and 17.6 mg per L expression volume, after protein L-affinity chromatography, size-exclusion chromatography and dialysis, of each MATCH protein, which compared favorably to a parental, full-length rabbit anti-TNFα IgG expressed and purified via similar methods (Table 3). DSF assays ($n = 2$ each) revealed average MATCH protein melting temperatures (mean Tm°C ± SD: pMATCH = 68.5 ± 0.3; apMATCH = 68.0 ± 0.1; apMATCH-diS = 69.4 ± 0.0) that suggested good protein stability

Table 2. Antigen-binding kinetics of anti-TNFα scFv variants as determined by SPR analysis.

	k_{on} (1/M·s)	k_{off} (1/s)	K_D (M)
aTNFα-scFv	3.95×10^5	1.05×10^{-4}	2.65×10^{-10}
aTNFα-scFv-λcap	4.19×10^5	9.41×10^{-5}	2.25×10^{-10}
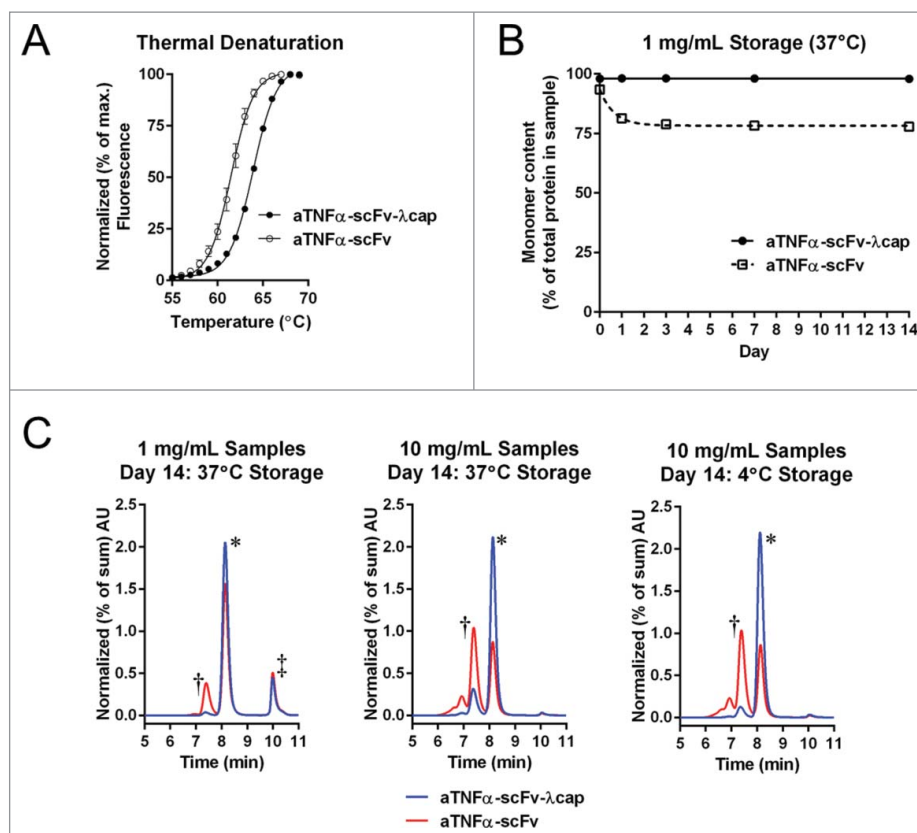
Figure 5. Improved thermal- and storage-stability of rabbit antibodies humanized with a λcapped $V_\kappa 1$-$V_H 3$-consensus scFv framework. (A) Thermal unfolding curves of each scFv variant fitted with the Boltzmann equation to data points (n=3 ; mean ± SD) generated in a DSF assay. (B) Maintenance of scFv monomer content (% of total protein content) during 2-week storage at 37°C; data points (n=3) reflect mean ± SD. (C) SE-HPLC chromatograms of exemplary protein samples at the indicated concentrations and after storage at the indicated durations/temperatures; scFv monomer (*), scFv dimer (†) and buffer matrix (‡) peaks are indicated.

(Fig. 7B). Additionally, analysis of gels containing non-reduced apMATCH-diS samples revealed a discrete band near the estimated weight of the heterodimer (~106 kDa), supporting inter-MATCH chain associations (Fig. 7A). Efficient MATCH chain dimerization was further demonstrated by the homogeneity of the protein content in protein L-purified samples analyzed by SE-HPLC (Fig. 7D). This homogeneity was largely retained even after storage of samples at 37°C for 28 d (Fig. 7C-D).

SPR analysis revealed that the antigen affinities of the Fvs in the MATCH formats closely resemble those of scFvs and single-chain diabodies (scDbs), including the MATCH Fvs positioned in the dimer-forming core, whose binding activity we suspected, and later demonstrated (described below), is dependent upon cognate dimerization (i.e., those displayed by the dimer-forming Fvs targeting TNFα and CD3ε, respectively) (Table 4). Additionally, each of the 3 tetraspecific molecules was capable of binding all 4 target antigens simultaneously, irrespective of the order of antigen-encounter, as demonstrated by SPR analysis of immobilized MATCH protein (Fig. 8 & Table S2).

Preferential cognate pairing of MATCH subunits

It is important to acknowledge that while our initial data suggest proper inter-MATCH chain assembly, they do not necessarily indicate the absence of non-cognate variable domain associations, specifically the inverted heterodimerization of MATCH chains that would produce chimeric CDR sets. It has been suggested that CDR sets influence the efficiency of V_L/V_H been

pairing,[48] and our SE-HPLC, SDS-PAGE and SPR data suggest that cognate pairing of MATCH chains is highly favored. In an attempt to quantitate the degree of inverted heterodimerization, we performed a SE-HPLC analysis of antibody and antibody-antigen complexes after incubation of the MATCH proteins with a molar equivalent of trimeric TNFα (i.e., 3-fold excess TNFα epitope). When applying this method of analysis to the parental anti-TNFα scFv used in the dimer-forming core domain of all MATCH formats (Fig. S1), SE-HPLC traces revealed convoluted peaks consistent with distinct antibody-antigen complex populations, reflecting the disparate sizes of 1:1, 2:1 and 3:1 scFv:TNFα complexes. Additionally, a peak whose retention time was consistent with the presence of residual, non-complexed TNFα in solution was observed, whereas non-complexed scFv was seemingly absent from solution, thus validating the application of this method[29] to identify inactive anti-TNFα antibody.

Separation of MATCH protein and MATCH-antigen complexes was less efficient due to the larger molecular weight range of the different protein populations. However, our results (Fig. 9) also clearly revealed the presence of 3 MATCH-TNFα complex populations and residual, non-complexed TNFα. Additionally, a slight "shouldering" of the 1xMATCH:TNFα complex peaks was observed, which could be explained by the presence of unbound MATCH protein. To estimate the proportion of unbound MATCH protein in solution, a deconvolution of the peaks was performed using PeakFit® v.4.12 software, assuming a tailed distribution for
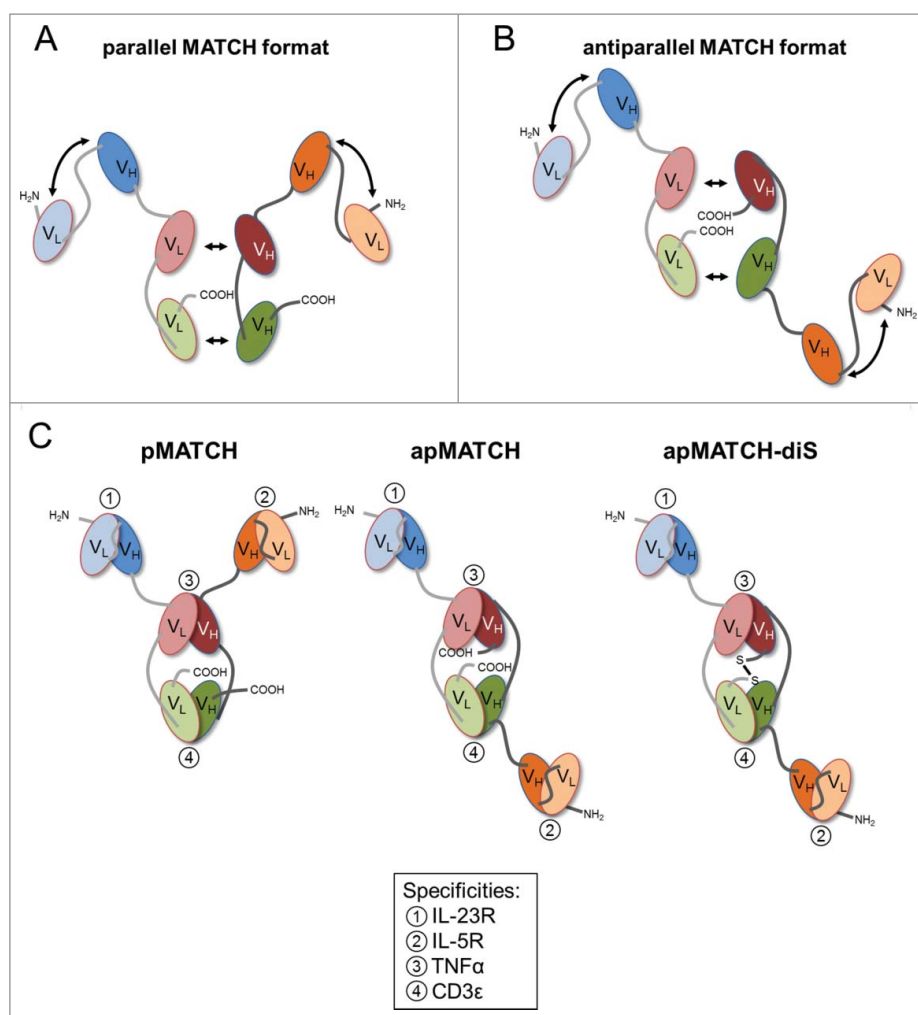
Figure 6. MATCH format concept and MATCH protein designs. (A) Orientation of the MATCH chains in the parallel MATCH format. The two-sided arrows indicate the variable domains whose interaction would represent a cognate association. In the context of MATCH proteins, the term "parallel" indicates that the split, heterodimer-forming variable domains on each chain are organized in the same N-term–C-term order as their cognate variable domains on the complementary MATCH chain. (B) Orientation of the MATCH chains in the antiparallel MATCH format. The two-sided arrows indicate the variable domains whose interaction would represent a cognate association. In the context of MATCH proteins, the term "antiparallel" indicates that the split, heterodimer-forming variable domains on each chain are organized in the opposite N-term-C-term order as their cognate variable domains on the complementary MATCH chain. (C) General designs of the MATCH proteins developed for the research described in this paper.

each peak and plotted to optimize goodness-of-fit (Fig. 9). This analysis estimated the proportion of unbound MATCH protein to be between 6.6 and 10.7% (apMATCH-diS < apMATCH < pMATCH) of total protein content, possibly indicating the maximal levels of non-cognate MATCH chain pairings. Meanwhile, to rule out any ability of non-cognate Fvs to complex with TNFα, we also created mispaired scFvs displaying the CDR sets that would theoretically arise from inverted heterodimerization of MATCH chains. These mispaired scFvs demonstrated no capacity to form complexes with TNFα in solution (Fig. S1C). This confirms that cognate dimerization of MATCH chains is highly favored, particularly in the antiparallel format.

As an additional proof of the efficiency of MATCH protein assembly, we designed a fourth MATCH protein variant (apMATCH-dis(IF)) (Fig. 10A), wherein we mutated a residue in each variable domain framework (V_L: G141C and V_H: G50C) of the heterodimer-forming anti-CD3ε Fv such that it would include a disulfide bridge at the interface of the cognate variable domains. Under this design, the

formation of an inter-chain disulfide bridge is entirely conditional on proper assembly of the MATCH protein chains. The apMATCH-diS(IF) was produced at comparable yields (14.1 mg per L expression volume) to the other MATCH proteins. SE-HPLC chromatograms of protein samples suggested a highly homogenous product (Fig. 10D) with a melting temperature (Tm°C ± SD: 68.5 ± 0.1) consistent with what was observed previously (Fig. 10C). Despite the amino-acid substitution in the variable domain frameworks of the anti-CD3ε Fv, the molecule maintained affinity for human CD3ε (K_D (M): 3.39×10^{-8}), and it showed good storage stability, with a 1 mg/mL sample losing only 3.4% of its heterodimer content after 2-week storage at 37°C (Fig. 10E). Crucially, SDS-PAGE gels show that non-reduced samples display a discrete band at the estimated position of the apMATCH-diS(IF) heterodimer, suggesting high dimerization efficiency (Fig. 10B). This finding was reflected in our TNFα-complexing analysis, which again revealed that production samples contain >90% active MATCH protein (Fig. 10F).
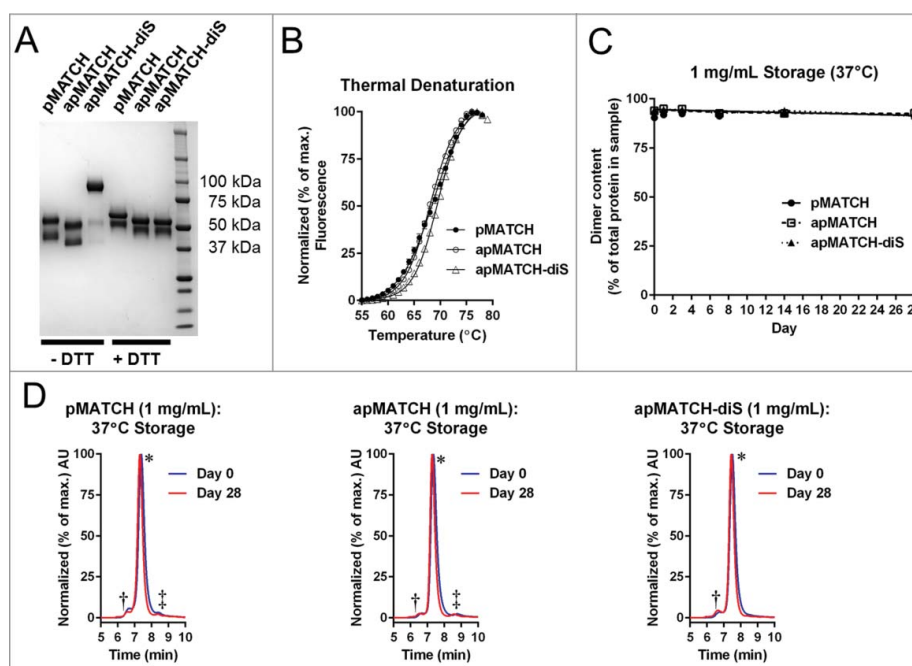
Figure 7. MATCH proteins can be expressed and purified and exhibit good thermal- and storage-stability. (A) Coomassie-stained SDS-PAGE gel reveals successful co-expression of each ~50 kDa MATCH chain. Additionally, non-reduced samples of the MATCH variant with additional C-terminal cysteines, apMATCH-diS, contain a protein near the expected gel position (~106 kDa) of heterodimeric MATCH protein. (B) Thermal unfolding curves of each MATCH protein fitted with the Boltzmann equation to data points (n=2 ; mean ± SD) generated in a DSF assay. (C) Each MATCH protein (n=1) largely retains its dimer content (% of total protein content) when stored at 1 mg/mL at 37°C, even for a period of 28 d (D) SE-HPLC chromatograms of 1 mg/mL samples of MATCH proteins at day 0 and day 28 of storage at 37°C; MATCH dimer (*), MATCH aggregate (†) and low-molecular-weight impurity (‡) peaks are indicated.

Discussion

Multispecific antibody formats provide the ability to produce single molecules that simultaneously recognize multiple protein sites with the high affinity that is characteristic of antibody paratopes. This can enable the highly selective cross-linking of multiple proteins, protein domains or cell-types to produce novel mechanisms of action or enhanced molecular pharmacokinetic properties. The arrival of bispecific antibodies on the market,[15,16] and the growing number of bispecifics undergoing clinical trials,[17] has confirmed the therapeutic value of this emerging class of biologics. These trends have led to a concurrent growth in the number of novel multispecific designs.[4,17,49] Most multispecific formats that have been described utilize either IgG-like designs (e.g., CrossMab[50] and DVD-IgG[46] formats) or exclusively combine multiple antibody fragments (e.g., bispecific T-cell engager (BiTE),[51] DART[52] and TandAb[53] formats).

While the production of some tri- and tetraspecific antibody formats, such as the TriMAb,[18] the tribody,[21] the triplebody[19]

and the 4-in-one CrossMab[54] has been described, these possess several limitations that must be considered. First, conventional heteromultimeric tri- and tetraspecifics include a multimerization domain(s), adding molecular weight and therefore reducing potential tissue distribution.[55] Moreover, all of these formats rely on the display of Fvs, which often exhibit poor stability and promote aggregation of the composite molecule.[24,56] Hence, other antibody formats that employ alternative binding moieties have been developed, such as Zybodies[57] and Fynomabs.[7] Variable-domain-only multispecifics with >2 specificities, such as the triplebody, have only been described in single-chain formats and only up to 3 specificities.

Heterodimeric tetraspecifics have, to our knowledge, never been described in the literature. However, such formats, provided they have at least one specificity on each of the individual subunits, would enable the highly efficient optimization of binding domain combinations in the final format through simple permutation of the subunit-expressing plasmids. Meanwhile, some capacity to produce such tetraspecifics in low-molecular-weight assemblies offers the flexibility to improve drug tissue penetration, where necessary. The efficient production of heterodimeric tetraspecifics whose assemblies are driven exclusively by interactions between antibody variable domains would introduce a novel platform that enhances the versatility and flexibility of multispecific technology. Unfortunately, the instability and aggregation propensity of variable domains is a substantial obstacle to the development of such formats. Additionally, production samples of multispecifics, particularly heterodimeric multispecifics, often contain several impurities due to unwanted subunit associations, supporting the need for redesigning mechanisms of subunit assembly to improve yields.

Table 3. Production yields of MATCH protein variants and a parental, rabbit IgG after chromatography and dialysis. The MATCH proteins and rIgG were expressed by transient gene expression in CHO and purified by similar methods.

Protein	Weight (Da)	Yield (mg) per L expression volume	Molar equivalents
pMATCH	106'822	3.4	0.18
apMATCH	105'219	12.1	0.65
apMATCH-diS	105'713	17.6	0.94
anti-TNFα rIgG	147'809	26.2	1

Table 4. Antigen-binding kinetics (determined by SPR analysis) of MATCH proteins as well as the scFv (PRO205 and PRO128) and scDb (PRO187) variants of the parental antibodies that provided the CDR set sequences for the MATCH proteins.

|	TNFα			CD3ε			IL-23R			IL-5R		
	k_{on} (1/M·s)	k_{off} (1/s)	K_D (M)	k_{on} (1/M·s)	k_{off} (1/s)	K_D (M)	k_{on} (1/M·s)	k_{off} (1/s)	K_D (M)	k_{on} (1/M·s)	k_{off} (1/s)	K_D (M)
pMATCH	2.23×10^5	6.84×10^{-4}	3.07×10^{-10}	1.10×10^5	2.21×10^{-3}	2.01×10^{-8}	5.29×10^5	3.46×10^{-4}	6.54×10^{-10}	1.89×10^6	1.94×10^{-4}	1.03×10^{-10}
apMATCH	3.58×10^5	7.63×10^{-4}	2.14×10^{-10}	3.50×10^5	2.50×10^{-3}	7.14×10^{-9}	1.10×10^6	3.75×10^{-4}	3.41×10^{-10}	1.76×10^6	2.22×10^{-4}	1.26×10^{-10}
apMATCH-diS	3.51×10^5	1.27×10^{-4}	3.61×10^{-10}	3.18×10^5	2.12×10^{-3}	6.69×10^{-9}	9.15×10^5	3.27×10^{-4}	3.58×10^{-10}	1.21×10^6	1.55×10^{-4}	1.28×10^{-10}
PRO205	5.51×10^5	1.44×10^{-4}	2.61×10^{-10}									
PRO187*				2.44×10^5	2.24×10^{-3}	9.21×10^{-9}				2.38×10^6	3.06×10^{-4}	1.29×10^{-10}
PRO128							1.45×10^6	2.67×10^{-4}	1.84×10^{-10}			
*scDb												

Figure 8. Each MATCH protein can bind all 4 of its target antigens simultaneously, irrespective of the order of antigen-encounter. The images in this figure depict sensor-gram data from an SPR analysis in which MATCH proteins were immobilized in individual channels on a sensor chip and each recombinant antigen was sequentially injected over the sensor chip channels at the time, and in the order, indicated on the x-axis of each graph.

We first sought to address the issue of Fv-instability with the ultimate aim of producing stable, non-aggregating variable-domain-only tetraspecifics. Researchers have previously observed a capacity of λ-derived V_L FWs to form highly stable Fv variants of hu4D5–8.[58] Importantly, incompatibility between the λ-derived FW and the κ-like 4D5-8 CDR sets necessitated affinity-damaging mutations to enable production of Fvs with a λ-derived V_L.[58] However, we suspected that replacement of a single FW region of a κ-derived V_L with the corresponding position of a V_λ germ-line sequence might confer the stability-enhanced features of V_λ-bearing Fvs without

requiring compatibility-promoting mutations to functionally critical, κ-derived CDR sets. Such a substitution has the added benefit that it still results in an Fv in which every FW region consists of an uninterrupted human sequence, theoretically reducing the risk of immunogenicity.

To our thinking, V_L FW IV represented a likely mediator of Fv instability, as it is positioned at the junction between variable and constant domains and appears to exhibit considerable structural diversity across antibody variants with identical CDR sets.[31] Our analysis of hu4D5–8 variant crystal structure overlays supported unnatural solvent-exposure at this position in
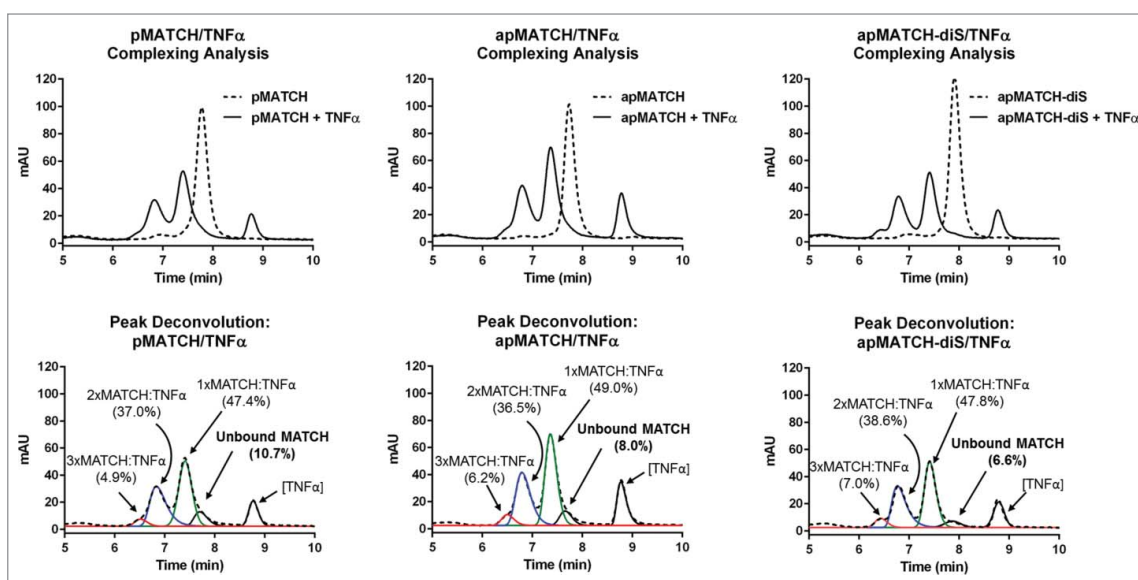
Figure 9. MATCH protein-TNFα complexing analysis suggests that bound MATCH protein comprises ≥89 % of reaction samples. The overlaid SE-HPLC chromatograms of MATCH protein alone (hashed line, top graphs) and MATCH protein after a 2-hour incubation with excess human TNFα (solid line, top graphs) suggests that a considerable majority of MATCH protein in solution is active insofar as the peak attributable to dimeric MATCH protein is largely absent after reacting with the antigen, and new peaks attributable to higher-molecular-weight complexes appear. After deconvoluting the chromatograms of the MATCH protein-TNFα reaction mixtures with PeakFit® v.4.12 software, our best estimates place the percentage of unbound MATCH protein between 6.6 and 10.7% (bottom graphs).
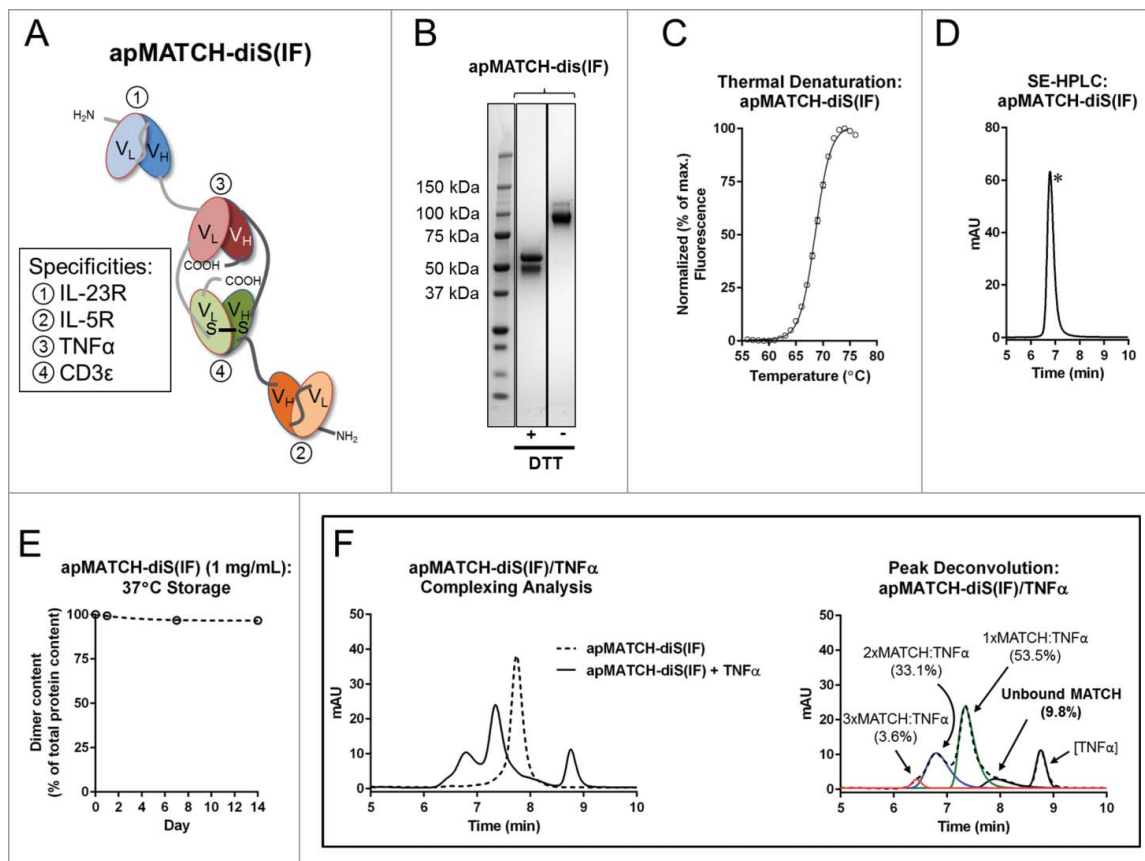
Figure 10. Functional MATCH protein variant with an inter-cognate-domain disulfide bridge is expressed and purified with comparable efficiency to classical MATCH proteins. (A) The design of apMATCH-diS(IF), which contains a framework mutation to both V_H and V_L domains of the anti-CD3ε, heterodimer-forming Fv that establishes an intra-Fv disulfide bridge. (B) Coomassie-stained SDS-PAGE gel supports the formation of heterodimeric apMATCH-diS(IF) in coexpression supernatants. The non-reduced protein sample contains a discrete protein band with the approximate electrophoretic mobility of the ~106 kDa MATCH protein heterodimer, whereas reduced samples possess 2 discrete bands at the approximate weight (~50 kDa) of the respective MATCH chains. (C) Thermal unfolding curve of apMATCH-diS(IF) fitted with the Boltzmann equation to data points ($n=3$; mean ± SD) generated in a DSF assay. (D) An SE-HPLC chromatogram of purified apMATCH-diS(IF) indicates that production samples can be prepared at very high purity; MATCH dimer (*) peak is indicated. (E) During 14-day storage at 37°C, the purity of MATCH dimer is largely maintained. (F) apMATCH-diS(IF)/TNFα complexing experiments are largely consistent with what was observed with classical MATCH proteins – bound MATCH dimer appears to comprise ≥90 % of MATCH protein in complex samples.

the Fv format. By applying λcap technology, i.e., replacement of V_κ FW IV with a V_λ FW IV germ-line sequence, we were able to stabilize humanized scFvs displaying both murine and rabbit CDR sets.

Humanized scFvs that employ λcap technology exhibited identical antigen-affinities to their unmodified counterparts, and they displayed higher thermal stability, a lower propensity toward concentration-induced aggregation, and were less prone to oligomerization during storage at stress temperatures. Because aggregation of antibodies is mediated by local unfolding events, resulting in the solvent-exposure of aggregation "hot spots,"[56] we were confident that such stability-enhanced Fvs could be combined to produce stable, non-aggregating variable-domain-only multispecific formats. Indeed, we observed high storage stability among our bispecific scDbs containing λcapped Fvs, as well as a resistance to proteolytic digestion for up to 7 d in human serum *in vitro* (data not shown). However, we must acknowledge that susceptibility to proteolytic digestion is likely to vary between CDR sets. As such, an evaluation of protein stability in serum should be applied on a molecule-by-molecule basis. The consistent stability and functionality of λcapped Fv-modules in bi- and trispecifics encouraged us to

employ them in the development of the novel tetraspecific formats described here, i.e., the MATCH formats.

We were able to produce the pMATCH, apMATCH, and apMATCH-diS proteins to a high purity, with yields of the latter approaching the molar equivalent of a parental rabbit IgG. Additionally, these proteins exhibited high thermal stability and were largely resistant to aggregation during storage. Critically, these proteins evinced comparable affinities for the target antigens as each of their individual, respective paratopes displayed in scFv or scDb formats. Moreover, each MATCH protein was able to simultaneously bind soluble forms of all 4 target antigens, irrespective of the order of antigen-exposure.

One of the challenges plaguing the production of heterodimeric multispecifics is the impurities that arise in production samples due to unwanted subunit associations. Existing variable-domain-only heterodimeric bispecifics, such as diabodies[28] and TandAbs,[53] apply a "V_L-linker-V_H" design to each subunit, with complementary variable domains being split between the 2 respective subunits. To prevent intra-subunit associations between non-complementary variable domains, such formats require that the peptide linker between tandem variable domains be ≤10 amino acids in length, theoretically restricting

molecular flexibility. Additionally, this design can result in the production of homodimers formed from the same unwanted non-cognate associations occurring between identical subunits, and techniques to enhance the efficiency of cognate pairing frequently rely on affinity-altering mutations to variable domains.[29]

By employing a "V_L-linker-V_L" and "V_H-linker-V_H" layout for the dimer-forming core of respective MATCH protein subunits, we effectively mitigated the risk of intra-subunit associations between split variable domains, enabling the incorporation of a lengthier peptide linker between said domains. Indeed, the pMATCH variant described in the present study included a linker length of 15 amino acids. Such length may be of considerable value to executing mechanisms of action that require greater protein flexibility.

Additionally, the design of the MATCH subunit core prevents the formation of homodimers driven by the dimer-forming split variable domains. There is only one variable domain per MATCH subunit available for the kind of non-complementary assembly that would lead to the production of homodimers, and this is contained in the peripheral scFv. This simple adjustment to the conventional heterodimer subunit assembly strategy likely eliminates homodimeric impurities that can arise during production and eases restrictions on intra-subunit linker lengths.

Theoretically, impurities could arise in MATCH production samples in the form of "inverted" MATCH heterodimers. In other words, the mispairing of dimer-forming split variable domains at the MATCH core might occur, producing a separate MATCH heterodimer population wherein the desired orientation of MATCH subunits is inverted. However, our complexing analysis suggests that ≥89 % of MATCH heterodimer in expression supernatants is properly assembled and fully reactive. The apMATCH-diS variant assembly was particularly efficient, with ~94% active protein in production samples and production yields comparable to a full-length IgG.

These findings are consistent with other research suggesting that CDR sets greatly influence the efficiency of variable domain assembly.[48] This is a likely reason why Zhu et al. described higher-than-expected efficiency of bispecific diabody heterodimerization during production.[59] However, after employing very similar purification and analytical techniques, those researchers found that their production samples consisted of ~75% active bispecifics,[59] considerably lower than the percentage of functional, tetraspecific MATCH in our production samples. This was the case even for the pMATCH variant with a peptide linker between the dimer-forming tandem split variable domains that was 3x longer than that of the diabody. Finally, production and analysis of the apMATCH-diS(IF) variant in the present study supports the idea that appropriate MATCH-subunit pairing is a highly efficient process, with its analytical outputs closely resembling those of the other variants with unmodified variable domains.

There are some obvious differences in the design of MATCH proteins and diabodies, which may account for some of the disparities in assembly specificity. These include the presence/absence of peripheral scFvs as well as the potential for homodimerization of subunits during expression. The latter would be especially problematic for diabodies if uneven subunit expression should occur. However, we feel that the most likely driver of V_L/V_H association specificity is the incompatibility of non-cognate CDR sets. A number of CDR positions are known to participate in the V_L/V_H interface,[31] and amino acid differences at these positions would likely disfavor associations between non-complementary variable domains. It is reasonable, then, to suspect that assembly specificity may vary across MATCH proteins containing different dimer-forming Fvs.

With that in mind, the successful production of the apMATCH-diS(IF) variant inspires confidence that dimer-forming Fvs can accommodate mutation that might enhance dimerization efficiency without compromising functionality. Alternatively, the screening of multiple dimer-forming Fvs for optimal MATCH assembly specificity (in the final format) could be employed. To further evaluate means to improve efficiency of cognate variable domain-pairing, we produced 2 MATCH variants with knob-into-hole mutations[29] to the dimer-forming Fvs (MATCH-KiH variants), aiming to increase the proportion of active MATCH protein in production samples. Crucially, the modified Fvs in these variants retained the affinity profiles of the unmodified Fvs (data not shown). After subjecting the MATCH-KiH variants to the same TNFα-complexing analysis described here, we did not observe an improvement in the levels of unbound MATCH protein compared to MATCH variants with unmodified domains (data not shown). However, in the event that different CDR sets in the dimer-forming MATCH Fvs would produce less specific V_L/V_H assemblies, these kinds of assembly-enhancing modifications could be explored to improve yields.

The value of tetraspecificity is not merely theoretical. Indeed four-in-one CrossMabs selectively targeting EGFR, HER2, HER3 and VEGF showed superior antitumor activity in multiple cancer models *in vivo* relative to effective combinations of bispecifics, and they did so at lower antibody concentrations.[54] The researchers surmised that these uniquely potent effects at lower concentrations were enabled by higher-avidity binding of tumor cells through interaction with several tumor-associated antigens (TAAs).[54] Under a different design, an antibody-based multispecific could be equipped with specificities for 2 TAAs to promote tumor-cell avidity while also displaying a T-cell-engaging paratope, theoretically enhancing the selectivity of T cell engaging antibodies.

For example, the EGFR-targeting BiTE described by Lutterbuese et al.[60] exhibited toxicity at higher concentrations due to drug interactions with healthy, EGFR-expressing cells. By adding a specificity for a co-expressing TAA, such as IGFR,[61] and carefully calibrating the affinities of the anti-TAA paratopes to maximize tumor-cell selectivity, one could reduce such adverse effects. With a fourth paratope, such a molecule could also target a preservative protein, such as human serum albumin (HSA), to lengthen serum half-life and reduce the frequency of drug administration.

It is important to reiterate that applications of the λcap-stabilized Fvs are not limited to MATCH formats or other tetraspecific molecules. λcapped Fvs may also be used in the production of stable scDbs and Fab-scFv fusion proteins. Such stability-enhanced Fvs could also be of considerable value to the production of other multispecifics that also rely on the

incorporation of Fvs for full functionality such as diabodies,[28] triplebodies[19] and Morrison formats.[62]

With the MATCH format, we have overcome many of the limitations in the production, stability and design-flexibility associated with conventional multispecific antibody fragment-based formats. This should provide researchers with an improved capacity to proceed from concept to clinic with molecules that target multiple cell-type-specific antigens, theoretically endowing us with drug candidates possessing ideal levels of selectivity and unique functionalities.

Materials and methods

Unless stated otherwise, general reagents were purchased from Axonlab.

scFv expression and purification

Recombinant amino acid sequences were *de novo* synthesized and cloned into an expression vector adapted from a pET26b (+) backbone (Novagen, Cat. #: 69862–3), and the resulting construct was used to transform BL12 (DE3) *E. coli* cells (Novagen, Cat. #: 69450), and scFv expression was induced with 1 mM IPTG (Cat. #: A 4773). Cells were harvested by centrifugation and resuspended in Wash Buffer (50 mM Tris-HCl (Cat. #: A1086), pH 7.5, 100 mM NaCl (Carl Roth, Cat. #: 9265), 5 mM EDTA (Cat. #: A 1104), and 1M urea (Sigma-Aldrich, Cat. #: 15604)) with 2% Triton X-100 (Cat. #: A1388), and the cell slurry was supplemented with 1 mM dithiothreitol (DTT, Cat. #: A2948), 0.1 mg/mL lysozyme (Cat. #: A 3711), 10 mM leupeptin (Cat. #: A 2183), 100 μM PMSF (Cat. #: A 0999) and 1 μM pepstatin (Cat. #: A 2205). The cells were then lysed by 3 cycles of ultrasonic homogenization, 0.01 mg/mL DNAse I (Cat. #: A 3778) was added and the homogenate was rotated for 20 min at room temperature (RT). The sample was then centrifuged at 15,000 g for 15 min, and the pellet was resuspended in fresh Wash Buffer. This procedure was performed 3x using Wash Buffer with 2% Triton X-100 and 2x using Wash Buffer without Triton X-100. After a final centrifugation step, the inclusion bodies (IBs) in the pellet were then solubilized in IB Solubilization Buffer (100 mM Tris-HCl, pH 8.0, 6M Gdn-HCl (Cat. #: A1499), 2 mM EDTA) at a ratio of 1.0 mL per 0.1 g of pellet and rotated for 30 min at RT. Subsequently, 50 mM DTT was added to the solution for an additional 30-min incubation at RT. Insoluble material was removed by centrifugation at 15,000 g for 10 min.

The refolding of the scFvs was performed by rapid dilution to a final protein concentration of 0.5 g/L in Refolding Buffer (100 mM Tris-HCl pH 8.0, 4.5 M urea, 3 mM cysteine (Cat. #: A3694), 3 mM cystine (Cat. #: A 1703), 400 mM arginine-HCl (Cat. #: A 1700)). The refolding reaction was incubated for 48 h at 4°C with constant stirring. The refolded proteins were purified by affinity chromatography with Capto L (GE Healthcare, Cat. #: 17–5478–01) on an ÄKTA protein purifier (GE Healthcare) at RT and eluted with 0.1 M glycine-HCl (Cat. #: A 3707), pH 2.8, followed by the rapid adjustment of sample pH with the addition of 180 μL 1 M Tris-HCl, pH 7.5 per 3 mL eluate. Where needed, elution pools were polished by size-exclusion chromatography on a Superdex 75 column (GE Healthcare,

Cat. #: 28989333) at RT. The isolated monomer fraction was analyzed by SE-HPLC, SDS-PAGE and UV/Vis spectroscopy. The resulting protein solution was concentrated and buffer exchanged by diafiltration with Native Buffer (150 mM NaCl, 50 mM citrate-phosphate, pH 6.4). Unless otherwise indicated, samples were kept on ice or at 4°C during all scFv purification steps.

SE-HPLC analysis

Samples were passed through either a Shodex™ (Showa Denko, Cat. #: 554–1740) KW402.5–4F column (for scFv analysis) or a Shodex™ (Showa Denko, Cat. #: 554–1741) KW403–4F column (MATCH protein analysis) with running buffer (Shodex™ KW402.5–4F: 250 mM NaCl, 50 mM NaOAc (Cat. #: A 1045), pH 6.0; Shodex™ KW403–4F: 35 mM NaH_2PO_4 (Cat. #: A 3905), 15 mM Na_2HPO_4 (Cat. #: A1372), 300 mM NaCl, pH 6.0) at a flow rate of 0.35 mL/min. Eluted protein was detected by absorbance at λ=280 nm.

The SE-HPLC columns were calibrated by separation of a protein standard mixture (Sigma-Aldrich, Cat. #: 69385) and plotting of the logarithm of the molecular weight versus the retention time. Apparent molecular weights for the recorded protein species were interpolated from the respective retention times and the exponential regression fit of the calibration curve.

Affinity determinations

Antigen affinities of hu4D5–8 scFv variants, MATCH proteins and MATCH parental scFvs/scDbs were determined by SPR using a MASS-1 SPR instrument (Sierra Sensors) and the following recombinant proteins (antigens): HER2 (Sino Biological, Inc., Cat. #: 10004-HCCH), CD3ε (Sino Biological, Inc., Cat. #: CT026-H0323H), IL-5R (R&D Systems, Cat. #: 253–5R), TNFα (Peprotech, Cat. #: 300–01A), IL-23R (Trenzyme, Accession #: NP_653302.2 – Gly24-Leu356 (custom synthesis)). Antigens were immobilized at 100–250 RUs on a sensor chip (SPR-2 Affinity Sensor High Capacity Amine, Sierra Sensors) using a standard amine coupling procedure. Affinity measurements were performed in HEPES Running Buffer (0.01 M HEPES (Sigma-Aldrich, Cat. #: 54457), 0.15 M NaCl, 0.05% Tween (Cat. #: A 4974)). For TNFα, a standard amine sensor was used. Two-fold serial dilutions of purified scFvs or MATCH proteins ranging from 0 to 90 nM were injected into the flow cells for 3 min (20 μl/min) and dissociation was allowed to proceed for 720 sec. After each injection cycle, surfaces were regenerated with a 45 second injection of 10 mM glycine-HCl pH 1.5. Affinities were calculated by fitting sensorgrams of at least 6 concentrations, and fits were considered accurate if Chi[2] was less than 10% of Rmax. Data were double-subtracted (reference channel and control cycle was subtracted).

Antigen-affinities of aTNFα-scFv-λcap, aTNFα-scFv, and apMATCH-diS(L/H) were determined by SPR analysis using a Biacore T200 System (GE Healthcare). Recombinant human CD3ε was directly coupled to a carboxymethylated dextrane surface on a CM5 sensor chip (GE Healthcare). Biotinylated human TNFα (ACROBiosystems, Cat. #: TNA-H8211) was coupled to a Biotin CAPture Kit, Series S Sensor Chip (GE

Healthcare). Production and analysis of sensorgram data using the Biacore T200 System was similar to that employed using the MASS-1 SPR instrument described above.

Thermal unfolding assays

The midpoint of transition for thermal unfolding of proteins was determined by DSF, as described by Niesen et al.[63] The DSF assay was performed in a qPCR machine (MX3005p, Agilent Technologies). The samples were diluted in buffer (citrate (Cat. #: A 3901) -phosphate pH 6.4, 0.15M NaCl) containing a final concentration of 5x SYPRO® orange (Lubio Science, Cat. #: S6650) in a total volume of 25 μL. Samples were measured in triplicates and evaluated while subjected to a programmed temperature ramp from 25–96°C.

Stress stability studies

Initial monomer (scFv) or dimer (MATCH protein) content of each sample was determined by SE-HPLC (d0). To calculate the percentage of total protein content that was mono-/multi-meric, the area under the curve peaking at the monomer (scFv) or dimer (MATCH) retention time was divided by the total area under curves not attributable to the sample matrix. The samples were stored at 37°C and analyzed repeatedly over a period of 2–4 weeks. Protein degradation was assessed by SDS-PAGE analysis, loading denatured proteins onto Mini-PROTEAN® TGX™ precast gels (Bio-Rad Laboratories, Cat. #: 4569036) and staining electrophoresed protein with Coomassie brilliant blue solution. The protein concentration was monitored at different time points by UV-Vis spectroscopy with an Infinite® M200 PRO microplate reader (Tecan Group, Ltd.).

MATCH expression and purification

The genes for each MATCH chain were *de novo* synthesized and cloned into a modified pcDNA3.1™/V5-His A (Thermo Fisher Scientific, Cat. #: V601020) expression vector. The proteins were expressed by transient gene expression with the CHO FreeStyle™ system (Thermo Fisher Scientific, Cat. #: K900020) and purified from CHO-S supernatants by protein L-affinity purification, capturing MATCH chains with Capto L resin (GE Healthcare) in a column affixed to an ÄKTA protein purifier (GE Healthcare) and eluted with 0.1 M citric acid, pH 2.0, followed by the rapid adjustment of sample pH with the addition of 0.4 mL 1 M Tris-HCl, pH 8.0 per 1 mL eluate. Protein solutions were then buffer exchanged with Native Buffer (150 mM NaCl, 50 mM citrate-phosphate, pH 6.4) using a PD-10 Desalting Column (GE Healthcare, Cat. #: 17–0851–01) and finally concentrated using a Vivaspin Protein Concentrator Spin Column (GE Healthcare, Cat. #: 28932223).

MATCH concomitant binding assays

The capacity of MATCH proteins to simultaneously bind all 4 of their target antigens was assessed by SPR analysis using a MASS-1 SPR instrument (Sierra Sensors). Each MATCH protein was diluted in 10 mM NaOAc, pH 5.0 to a final concentration of 5.0 μg/mL and immobilized on a sensor chip (SPR-2

Affinity Sensor High Capacity Amine, Sierra Sensors). Saturating concentrations of each antigen (CD3ε: 1′200 nM; IL-5R: 90 nM; IL-23R: 180 nM; TNFα: 90 nM) were sequentially injected, each for 3 min (20 μL/min), into sensor chip flow cells presenting immobilized MATCH protein or mock. As an additional control, sensor chip flow cells presenting immobilized MATCH protein were treated with buffer only for 3 min (20 μL/min) 4 times prior to initiating antigen injections (pre-antigen buffer injections), and the sensor chip responses were measured. Data were double-subtracted.

MATCH/scFv-TNFα complexing analysis

The requisite amount of MATCH protein or scFv was added to a solution containing 4.0 μg trimeric TNFα (Peprotech) to reach a molar equivalent between antibody and antigen (i.e., 3-fold excess of TNFα epitope). Solution volumes were adjusted to 20 μL by adding ddH$_2$O. Samples were incubated for 2 h at RT, agitating gently throughout. Reaction mixtures were then analyzed by SE-HPLC, passing each sample through either a Shodex™ KW402.5–4F column (for scFv-TNFα complexing analysis) or a Shodex™ KW403–4F column (for MATCH-TNFα complexing analysis) under the conditions described above. The MATCH-TNFα complexing reactions produced poorly separated elution curves in SE-HPLC chromatograms, complicating efforts to determine the proportions of protein and protein-complex populations in the samples. To estimate these proportions, raw data were analyzed in PeakFit v4.12, a deconvolution of the protein peaks was performed assuming a tailed distribution and optimizing goodness-of-fit (all R^2 values were $\geq$ 0.99).

Disclosure of potential conflicts of interest

Acknowledgments

References

1. Doppalapudi VR, Huang J, Liu D, Jin P, Liu B, Li L, Desharnais J, Hagen C, Levin NJ, Shields MJ, et al. Chemical generation of bispecific antibodies. Proc Natl Acad Sci U S A 2010; 107:22611-6; PMID:21149738; http://dx.doi.org/10.1073/pnas.1016478108

2. Lewis SM, Wu X, Pustilnik A, Sereno A, Huang F, Rick HL, Guntas G, Leaver-Fay A, Smith EM, Ho C, et al. Generation of bispecific IgG antibodies by structure-based design of an orthogonal Fab interface. Nat Biotechnol [Internet] 2014; 32:191-8. Available from: http://www.ncbi.nlm.nih.gov/pubmed/24463572; PMID:24463572; http://dx.doi.org/10.1038/nbt.2797

3. Liu Z, Leng EC, Gunasekaran K, Pentony M, Shen M, Howard M, Stoops J, Manchulenko K, Razinkov V, Liu H, et al. A Novel Antibody Engineering Strategy for Making Monovalent Bispecific Heterodimeric IgG Antibodies by Electrostatic Steering Mechanism. J Biol

Chem [Internet] 2015; 290:7535-62. Available from: http://www.jbc.org/content/290/12/7535.abstract; PMID:25583986; http://dx.doi.org/10.1074/jbc.M114.620260

4. Weidle UH, Tiefenthaler G, Weiss EH, Georges G, Brinkmann U. The intriguing options of multispecific antibody formats for treatment of cancer. Cancer Genomics and Proteomics 2013; 10:1-18; PMID:23382582

5. Smith AJ. New Horizons in Therapeutic Antibody Discovery: Opportunities and Challenges versus Small-Molecule Therapeutics. J Biomol Screen [Internet] 2014; 20:437-53. Available from: http://jbx.sagepub.com/cgi/doi/10.1177/1087057114562544; PMID:25512329; http://dx.doi.org/10.1177/1087057114562544

6. Spiess C, Zhai Q, Carter PJ. Alternative molecular formats and therapeutic applications for bispecific antibodies. Mol Immunol [Internet] 2015; 67:95-106. Available from: http://dx.doi.org/10.1016/j.molimm.2015.01.003; PMID:25637431; http://dx.doi.org/10.1016/j.molimm.2015.01.003

7. Brack S, Attinger-Toller I, Schade B, Mourlane F, Klupsch K, Woods R, Hachemi H, von der Bey U, Koenig-Friedrich S, Bertschinger J, et al. A Bispecific HER2-Targeting FynomAb with Superior Antitumor Activity and Novel Mode of Action. Mol Cancer Ther [Internet] 2014; 13:2030-9. Available from: http://www.ncbi.nlm.nih.gov/pubmed/24994770; PMID:24994770; http://dx.doi.org/10.1158/1535-7163.MCT-14-0046-T

8. Dong J, Sereno A, Snyder WB, Miller BR, Tamraz S, Doern A, Favis M, Wu X, Tran H, Langley E, et al. Stable IgG-like bispecific antibodies directed toward the type I insulin-like growth factor receptor demonstrate enhanced ligand blockade and anti-tumor activity. J Biol Chem [Internet] 2011; 286:4703-17. Available from: http://www.pubmedcentral.nih.gov/articlerender.fcgi?artid=3039382&tool=pmcentrez&rendertype=abstract; PMID:21123183; http://dx.doi.org/10.1074/jbc.M110.184317

9. Jost C, Schilling J, Tamaskovic R, Schwill M, Honegger A, Plückthun A. Structural basis for eliciting a cytotoxic effect in HER2-overexpressing cancer cells via binding to the extracellular domain of HER2. Structure 2013; 21:1979-91; PMID:24095059; http://dx.doi.org/10.1016/j.str.2013.08.020

10. Dennis MS, Zhang M, Gloria Meng Y, Kadkhodayan M, Kirchhofer D, Combs D, Damico LA. Albumin binding as a general strategy for improving the pharmacokinetics of proteins. J Biol Chem 2002; 277:35035-43; PMID:12119302; http://dx.doi.org/10.1074/jbc.M205854200

11. Yu YJ, Zhang Y, Kenrick M, Hoyte K, Luk W, Lu Y, Atwal J, Elliott JM, Prabhu S, Watts RJ, et al. Boosting brain uptake of a therapeutic antibody by reducing its affinity for a transcytosis target. Sci Transl Med 2011; 3:84ra44; PMID:21613623; http://dx.doi.org/10.1126/scitranslmed.3002230

12. Dennis MS, Watts RJ. Transferrin antibodies into the brain. Neuropsychopharmacology [Internet] 2012; 37:302-3. Available from: http://dx.doi.org/10.1038/npp.2011.196; PMID:22157868; http://dx.doi.org/10.1038/npp.2011.196

13. Yu YJ, Atwal JK, Zhang Y, Tong RK, Wildsmith KR, Tan C, Bien-Ly N, Hersom M, Maloney J a, Meilandt WJ, et al. Therapeutic bispecific antibodies cross the blood-brain barrier in nonhuman primates. Sci Transl Med [Internet] 2014; 6:261ra154. Available from: http://www.ncbi.nlm.nih.gov/pubmed/25378646\nhttp://stm.sciencemag.org/content/6/261/261ra154.full.pdf; PMID:25378646; http://dx.doi.org/10.1126/scitranslmed.3009835

14. Wunder A, Muller-Ladner U, Stelzer EH, Funk J, Neumann E, Stehle G, Pap T, Sinn H, Gay S, Fiehn C. Albumin-based drug delivery as novel therapeutic approach for rheumatoid arthritis. J Immunol [Internet] 2003; 170:4793-801. Available from: http://www.ncbi.nlm.nih.gov/pubmed/12707361; PMID:12707361; http://dx.doi.org/10.4049/jimmunol.170.9.4793

15. Topp MS, Kufer P, Gökbuget N, Goebeler M, Klinger M, Neumann S, Horst HA, Raff T, Viardot A, Schmid M, et al. Targeted therapy with the T-cell - Engaging antibody blinatumomab of chemotherapy-refractory minimal residual disease in B-lineage acute lymphoblastic leukemia patients results in high response rate and prolonged leukemia-free survival. J Clin Oncol 2011; 29:2493-8; PMID:21576633; http://dx.doi.org/10.1200/JCO.2010.32.7270

16. Linke R, Klein A, Seimetz D. Catumaxomab: Clinical development and future directions. MAbs 2010; 2:129-36; PMID:20190561; http://dx.doi.org/10.4161/mabs.2.2.11221

17. Spiess C, Zhai Q, Carter PJ. Alternative molecular formats and therapeutic applications for bispecific antibodies. Mol Immunol 2015; 67:95-106; PMID:25637431; http://dx.doi.org/10.1016/j.molimm.2015.01.003

18. Castoldi R, Jucknischke U, Pradel LP, Arnold E, Klein C, Scheiblich S, Niederfellner G, Sustmann C. Molecular characterization of novel trispecific ErbB-cMet-IGF1R antibodies and their antigen-binding properties. Protein Eng Des Sel 2012; 25:551-9; PMID:22936109; http://dx.doi.org/10.1093/protein/gzs048

19. Schubert I, Kellner C, Stein C, Kügler M, Schwenkert M, Saul D, Mentz K, Singer H, Stockmeyer B, Hillen W, et al. A single-chain triplebody with specificity for CD19 and CD33 mediates effective lysis of mixed lineage leukemia cells by dual targeting. MAbs 2011; 3:21-30; PMID:21081841; http://dx.doi.org/10.4161/mabs.3.1.14057

20. Kügler M, Stein C, Kellner C, Mentz K, Saul D, Schwenkert M, Schubert I, Singer H, Oduncu F, Stockmeyer B, et al. A recombinant trispecific single-chain Fv derivative directed against CD123 and CD33 mediates effective elimination of acute myeloid leukaemia cells by dual targeting. Br J Haematol 2010; 150:574-86; PMID:20636437; http://dx.doi.org/10.1111/j.1365-2141.2010.08300.x

21. Schoonjans R, Willems A, Schoonooghe S, Fiers W, Grooten J, Mertens N. Fab chains as an efficient heterodimerization scaffold for the production of recombinant bispecific and trispecific antibody derivatives. J Immunol 2000; 165:7050-7; PMID:11120833; http://dx.doi.org/10.4049/jimmunol.165.12.7050

22. Li Z, Krippendorff B-F, Sharma S, Walz AC, Lavé T, Shah DK. Influence of molecular size on tissue distribution of antibody fragments. MAbs [Internet] 2016; 8:113-9. Available from: http://www.ncbi.nlm.nih.gov/pubmed/26496429; PMID:26496429; http://dx.doi.org/10.1080/19420862.2015.1111497

23. Vossen ACTM, Tibbe GJM, Kroos MJ, van de Winkel JGJ. Fc receptor binding of anti-CD3 monoclonal antibodies is not essential for immunosuppression, but triggers cytokine-related side effects. Eur J Immunol 1995; 25:1492-6; PMID:7614975; http://dx.doi.org/10.1002/eji.1830250603

24. Röthlisberger D, Honegger A, Plückthun A. Domain interactions in the Fab fragment: A comparative evaluation of the single-chain Fv and Fab format engineered with variable domains of different stability. J Mol Biol 2005; 347:773-89; PMID:15769469; http://dx.doi.org/10.1016/j.jmb.2005.01.053

25. Wu H, Kroe-Barrett R, Singh S, Robinson AS, Roberts CJ. Competing aggregation pathways for monoclonal antibodies. FEBS Lett [Internet] 2014; 588:936-41. Available from: http://dx.doi.org/10.1016/j.febslet.2014.01.051; PMID:24530501; http://dx.doi.org/10.1016/j.febslet.2014.01.051

26. Zhou Y, Goenaga AL, Harms BD, Zou H, Lou J, Conrad F, Adams GP, Schoeberl B, Nielsen UB, Marks JD. Impact of Intrinsic Affinity on Functional Binding and Biological Activity of EGFR Antibodies. Mol Cancer Ther 2012; 11:1467-76; PMID:22564724; http://dx.doi.org/10.1158/1535-7163.MCT-11-1038

27. Rudnick SI, Adams GP. Affinity and avidity in antibody-based tumor targeting. Cancer Biother Radiopharm 2009; 24:155-61; PMID:19409036; http://dx.doi.org/10.1089/cbr.2009.0627

28. Holliger P, Prospero T. "Diabodies": Small bivalent and bispecific antibody fragments. Proc Natl Acad Sci U S A 1993; 90:6444-8; PMID:8341653; http://dx.doi.org/10.1073/pnas.90.14.6444

29. Zhu Z, Presta LG, Zapata G, Carter P. Remodeling domain interfaces to enhance heterodimer formation. Protein Sci 1997; 6:781-8; PMID:9098887; http://dx.doi.org/10.1002/pro.5560060404

30. Ewert S, Honegger A, Plückthun A. Stability improvement of antibodies for extracellular and intracellular applications: CDR grafting to stable frameworks and structure-based framework engineering. Methods 2004; 34:184-99; PMID:15312672; http://dx.doi.org/10.1016/j.ymeth.2004.04.007

31. Knappik A, Ge L, Honegger A, Pack P, Fischer M, Wellnhofer G, Hoess A, Wölle J, Plückthun A, Virnekäs B. Fully synthetic human combinatorial antibody libraries (HuCAL) based on modular consensus frameworks and CDRs randomized with trinucleotides. J Mol Biol 2000; 296:57-86; PMID:10656818; http://dx.doi.org/10.1006/jmbi.1999.3444

32. Eigenbrot C, Randal M, Presta L, Carter P, Kossiakoff AA. X-ray Structures of the Antigen-binding Domains from Three Variants of Humanized anti-p185HER2 Antibody 4D5 and Comparison with Molecular Modeling. J. Mol. Biol.1993; 229:969-95; PMID:8095303; http://dx.doi.org/10.1006/jmbi.1993.1099

33. Honegger A, Plückthun A. Yet another numbering scheme for immunoglobulin variable domains: an automatic modeling and analysis tool. J Mol Biol [Internet] 2001; 309:657-70. Available from: http://www.sciencedirect.com/science/article/pii/S0022283601946625; PMID:11397087; http://dx.doi.org/10.1006/jmbi.2001.4662

34. Rader C, Ritter G, Nathan S, Elia M, Gout I, Jungbluth AA, Cohen LS, Welt S, Old LJ, Barbas CF. The rabbit antibody repertoire as a novel source for the generation of therapeutic human antibodies. J Biol Chem 2000; 275:13668-76; PMID:10788485; http://dx.doi.org/10.1074/jbc.275.18.13668

35. Lavinder JJ, Hoi KH, Reddy ST, Wine Y, Georgiou G. Systematic characterization and comparative analysis of the rabbit immunoglobulin repertoire. PLoS One 2014; 9:1-11; PMID:24978027; http://dx.doi.org/10.1371/journal.pone.0101322

36. Borras LJ, Urech D. Humanization of rabbit antibodies using a universal antibody framework. U.S. Patent Number 8,293,235. Filed on June 25, 2009.

37. Borras L, Gunde T, Tietz J, Bauer U, Hulmann-Cottier V, Grimshaw JPA, Urech DM. Generic approach for the generation of stable humanized single-chain Fv fragments from rabbit monoclonal antibodies. J Biol Chem 2010; 285:9054-66; PMID:20056614; http://dx.doi.org/10.1074/jbc.M109.072876

38. Willuda J, Honegger A, Waibel R, Schubiger PA, Stahel R, Zangemeister-Wittke U, Plückthun A. High Thermal Stability Is Essential for Tumor Targeting of Antibody Fragments. Cancer Res 1999; 59:5758-67; PMID:10582696

39. Rosenberg AS. Effects of protein aggregates: an immunologic perspective. AAPS J 2006; 8:E501-7; PMID:17025268; http://dx.doi.org/10.1208/aapsj080359

40. Joubert MK, Hokom M, Eakin C, Zhou L, Deshpande M, Baker MP, Goletz TJ, Kerwin BA, Chirmule N, Narhi LO, et al. Highly aggregated antibody therapeutics can enhance the in vitro innate and late-stage T-cell immune responses. J Biol Chem 2012; 287:25266-79; PMID:22584577; http://dx.doi.org/10.1074/jbc.M111.330902

41. Lalor P, Nossal G, Sanderson R, McHeyzer-Williams M. Functional and molecular characterization of single, (4-hydroxy-3-nitrophenyl)acetyl (NP)-specific, IgG1+ B cells from antibody-secreting and memory B cell pathways in the C57BL/6 immune response to NP. Eur J Immunol 1992; 22:3001-11; PMID:1425924; http://dx.doi.org/10.1002/eji.1830221136

42. Lightwood DJ, Carrington B, Henry AJ, McKnight AJ, Crook K, Cromie K, Lawson ADG. Antibody generation through B cell panning on antigen followed by in situ culture and direct RT-PCR on cells harvested en masse from antigen-positive wells. J Immunol Methods 2006; 316:133-43; PMID:17027850; http://dx.doi.org/10.1016/j.jim.2006.08.010

43. Huston JS, Levinson D, Mudgett-Hunter M, Tai MS, Novotný J, Margolies MN, Ridge RJ, Bruccoleri RE, Haber E, Crea R. Protein engineering of antibody binding sites: recovery of specific activity in an anti-digoxin single-chain Fv analogue produced in Escherichia coli. Proc Natl Acad Sci U S A [Internet] 1988; 85:5879-83. Available from: http://www.pubmedcentral.nih.gov/articlerender.fcgi?artid=281868&tool=pmcentrez&rendertype=abstract; PMID:3045807; http://dx.doi.org/10.1073/pnas.85.16.5879

44. Brüsselbach S, Korn T, Völkel T, Müller R, Kontermann R. Enyzme recruitment and tumor cell killing in vitro by a secreted bispecific single-chain diabody. Tumor Target 1999; 4:115-23

45. Schaefer J V, Plückthun A. Transfer of engineered biophysical properties between different antibody formats and expression systems. Protein Eng Des Sel 2012; 25:485-505; PMID:22763265; http://dx.doi.org/10.1093/protein/gzs039

46. Wu C, Ying H, Grinnell C, Bryant S, Miller R, Clabbers A, Bose S, McCarthy D, Zhu R-R, Santora L, et al. Simultaneous targeting of multiple disease mediators by a dual-variable-domain immunoglobulin. Nat Biotechnol 2007; 25:1290-7; PMID:17934452; http://dx.doi.org/10.1038/nbt1345

47. Steinmetz A, Vallée F, Beil C, Lange C, Baurin N, Beninga J, Capdevila C, Corvey C, Dupuy A, Ferrari P, et al. CODV-Ig, a universal bispecific tetravalent and multifunctional immunoglobulin format for medical applications. MAbs [Internet] 2016; 8:867-78. Available from: http://dx.doi.org/10.1080/19420862.2016.1162932; PMID:26984268; http://dx.doi.org/10.1080/19420862.2016.1162932

48. Honegger A, Malebranche AD, Röthlisberger D, Plückthun A. The influence of the framework core residues on the biophysical properties of immunoglobulin heavy chain variable domains. Protein Eng Des Sel 2009; 22:121-34; PMID:19136675; http://dx.doi.org/10.1093/protein/gzn077

49. Kontermann RE, Brinkmann U. Bispecific antibodies. Drug Discov Today [Internet] 2015; 20:838-47. Available from: http://dx.doi.org/10.1016/j.drudis.2015.02.008; PMID:25728220; http://dx.doi.org/10.1016/j.drudis.2015.02.008

50. Schaefer W, Regula JT, Bähner M, Schanzer J, Croasdale R, Dürr H, Gassner C, Georges G, Kettenberger H, Imhof-Jung S, et al. Immunoglobulin domain crossover as a generic approach for the production of bispecific IgG antibodies. Proc Natl Acad Sci U S A 2011; 108:11187-92; PMID:21690412; http://dx.doi.org/10.1073/pnas.1019002108

51. Baeuerle PA, Reinhardt C. Bispecific T-cell engaging antibodies for cancer therapy. Cancer Res 2009; 69:4941-4; PMID:19509221; http://dx.doi.org/10.1158/0008-5472.CAN-09-0547

52. Moore PA, Zhang W, Rainey GJ, Burke S, Li H, Huang L, Gorlatov S, Veri MC, Aggarwal S, Yang Y, et al. Application of dual affinity retargeting molecules to achieve optimal redirected T-cell killing of B-cell lymphoma. Blood 2011; 117:4542-51; PMID:21300981; http://dx.doi.org/10.1182/blood-2010-09-306449

53. Kipriyanov SM, Moldenhauer G, Schuhmacher J, Cochlovius B, Von der Lieth CW, Matys ER, Little M. Bispecific tandem diabody for tumor therapy with improved antigen binding and pharmacokinetics. J Mol Biol [Internet] 1999; 293:41-56. Available from: http://www.sciencedirect.com/science/article/pii/S002228369993156X; PMID:10512714; http://dx.doi.org/10.1006/jmbi.1999.3156

54. Hu S, Fu W, Xu W, Yang Y, Cruz M, Berezov SD, Jorissen D, Takeda H, Zhu W. Four-in-one antibodies have superior cancer inhibitory activity against EGFR, HER2, HER3, and VEGF through disruption of HER/MET crosstalk. Cancer Res 2015; 75:159-70; PMID:25371409; http://dx.doi.org/10.1158/0008-5472.CAN-14-1670

55. Li Z, Krippendorff B-F, Sharma S, Walz AC, Lavé T, Shah DK. Influence of molecular size on tissue distribution of antibody fragments. MAbs 2016; 8:113-9; PMID:26496429; http://dx.doi.org/10.1080/19420862.2015.1111497

56. Wu H, Kroe-Barrett R, Singh S, Robinson AS, Roberts CJ. Competing aggregation pathways for monoclonal antibodies. FEBS Lett 2014; 588:936-41; PMID:24530501; http://dx.doi.org/10.1016/j.febslet.2014.01.051

57. LaFleur DW, Abramyan D, Kanakaraj P, Smith RG, Shah RR, Wang G, Yao X-T, Kankanala S, Boyd E, Zaritskaya L, et al. Monoclonal antibody therapeutics with up to five secificities: functional enhancement through fusion of target-specific peptides. MAbs 2013; 5:1-11; PMID:23254906; http://dx.doi.org/10.4161/mabs.23043

58. Ewert S, Huber T, Honegger A, Plückthun A. Biophysical properties of human antibody variable domains. J Mol Biol [Internet] 2003; 325:531-53. Available from: http://www.ncbi.nlm.nih.gov/pubmed/12498801\nhttp://linkinghub.elsevier.com/retrieve/pii/S0022283602012378; PMID:12498801; http://dx.doi.org/10.1016/S0022-2836(02)01237-8

59. Zhu Z, Zapata G, Shalaby R, Snedecor B, Chen H, Carter P. High level secretion of a humanized bispecific diabody from Escherichia coli. Nat Biotechnol 1996; 14:303-8; PMID:9630890; http://dx.doi.org/10.1038/nbt0296-192

60. Lutterbuese R, Raum T, Kischel R, Hoffmann P, Mangold S, Rattel B, Friedrich M, Thomas O, Lorenczewski G, Rau D, et al. T cell-engaging BiTE antibodies specific for EGFR potently eliminate KRAS- and BRAF-mutated colorectal cancer cells. Proc Natl Acad Sci U S A 2010; 107:12605-10; PMID:20616015; http://dx.doi.org/10.1073/pnas.1000976107

61. Vigneri PG, Tirr∫ E, Pennisi MS, Massimino M, Stella S, Romano C, Manzella L. The Insulin/IGF System in Colorectal Cancer Development and Resistance to Therapy. Front Oncol [Internet] 2015; 5:230. Available from: http://www.pubmedcentral.nih.gov/articlerender.fcgi?artid=4606066&tool=pmcentrez&rendertype=abstract; PMID:26528439; http://dx.doi.org/10.3389/fonc.2015.00230

62. Coloma MJ, Morrison SL. Design and production of novel tetravalent bispecific antibodies. Nat Biotechnol 1997; 15:159-63; PMID:9035142; http://dx.doi.org/10.1038/nbt0297-159

63. Niesen FH, Berglund H, Vedadi M. The use of differential scanning fluorimetry to detect ligand interactions that promote protein stability. Nat Protoc [Internet] 2007; 2:2212-21. Available from: http://www.nature.com/doifinder/10.1038/nprot.2007.321; PMID:17853878; http://dx.doi.org/10.1038/nprot.2007.321

64. Honegger A, Plückthun A. Yet another numbering scheme for immunoglobulin variable domains: an automatic modeling and analysis tool. J Mol Biol 2001; 309:657-70; PMID:11397087; http://dx.doi.org/10.1006/jmbi.2001.4662